Drug Design, Development and Therapy

Dovepress
Taylor & Francis Group

Open Access Full Text Article

ORIGINAL RESEARCH

In vivo Pharmacokinetic Interactions Between Palbociclib and Rivaroxaban or Apixaban: Implications for Increased Drug Exposure and Dose Adjustments

Wenyu Du[1,2], Zihan Liu[1,2,*], Ying Li[2,*], Zhi Wang[2], Zhanjun Dong[2]

[1]Graduate School, Hebei Medical University, Shijiazhuang, 050017, People's Republic of China; [2]Hebei General Hospital, Hebei Key Laboratory of Clinical Pharmacy, Shijiazhuang, 050051, People's Republic of China

*These authors contributed equally to this work

Correspondence: Zhanjun Dong, Email dzjhbgh@126.com

Background: Apixaban and rivaroxaban are oral direct factor Xa inhibitors, primarily eliminated through CYP3A4-mediated metabolism and direct intestinal excretion. Previous studies suggest that palbociclib, a CDK4/6 inhibitor, may increase the systemic exposure of these anticoagulants; however, the specific pharmacokinetic mechanisms remain unclear. This study aims to evaluate the effects of palbociclib on the pharmacokinetics of apixaban and rivaroxaban using a rat model to optimize combined drug regimens.

Methods: Male Sprague-Dawley rats were divided into eleven groups to assess interactions between palbociclib and either apixaban or rivaroxaban (n=6). Rats received single or combined doses of palbociclib (11 mg/kg), apixaban (0.25 or 0.5 mg/kg), or rivaroxaban (1 or 2 mg/kg), administered either simultaneously or with a 12-hour interval. Plasma drug concentrations were measured at multiple time points using UPLC-MS/MS, and pharmacokinetic parameters (AUC, C_{max}, $CL_{z/F}$, and $V_{z/F}$) were calculated. Additionally, mRNA expression levels of CYP3A4, P-glycoprotein and BCRP in liver and intestinal tissues were analyzed via qRT-PCR to elucidate the underlying interaction mechanisms.

Results: The results demonstrated that palbociclib significantly increased the exposure of both apixaban and rivaroxaban. Specifically, palbociclib elevated the AUC and C_{max} of apixaban by approximately two-fold (2.06-fold, $p = 0.006$ and 2.09-fold, $p = 0.006$) and rivaroxaban by nearly four-fold (3.81-fold, $p = 0.001$ and 3.75-fold, $p = 0.001$), while reducing their clearance and volume of distribution. Even at reduced doses, the exposure to apixaban and rivaroxaban remained disproportionately increased when co-administered with palbociclib. Conversely, administering apixaban or rivaroxaban 12 hours after palbociclib resulted in no significant pharmacokinetic changes.

Conclusion: The remarkable increased exposure of DOAC suggest that palbociclib likely enhance intestinal absorption mediated by decreased P-gp and BCRP expression, indicating markedly improved bioavailability for both drugs. These pharmacokinetic interactions provide valuable insights for optimizing dosing regimens of palbociclib in combination with apixaban or rivaroxaban, potentially reducing toxicity risks and enhancing the safety of co-administration in clinical settings.

Keywords: cancer-associated venous thromboembolism, palbociclib, apixaban, rivaroxaban, drug-drug interaction

Introduction

Cancer is frequently associated with a hypercoagulable state, which poses a significant public health challenge for patients. Cancer-associated venous thromboembolism (CAT), including deep vein thrombosis (DVT) and pulmonary embolism (PE), is the second leading cause of death among cancer patients, contributing to over 3 million fatalities annually worldwide.[1,2] Patients diagnosed with cancer have a markedly higher risk of developing venous thromboembolism (VTE), with estimates

Received: 4 October 2024
Accepted: 15 August 2025
Published: 25 August 2025

indicating a four- to sevenfold increase compared to individuals without cancer.[3] This elevated risk is driven by several factors, including the release of procoagulant substances by tumors, the effects of chemotherapy, and prolonged immobility or bed rest, all of which foster a hypercoagulable state in cancer patients.[4,5]

Despite advancements in cancer therapy, the incidence of VTE has been increasing in recent years.[6] Low-molecular-weight heparin (LMWH) has traditionally been the standard treatment for cancer-associated thrombosis. However, the requirement for daily subcutaneous injections and the associated high costs often result in reduced patient compliance, highlighting the need for safer and more convenient alternatives.[7,8]

Direct oral anticoagulants (DOACs) have emerged as a superior alternative, offering the convenience of oral administration, stable pharmacokinetics, and eliminating the need for frequent monitoring.[9] DOACs, including rivaroxaban, edoxaban, and apixaban, provide effective anticoagulation with a favorable risk-benefit profile, as demonstrated in multiple randomized controlled trials.[10–13] Nonetheless, gaps in research remain, particularly regarding the safety and efficacy of DOACs in specific cancer populations, such as patients with gastrointestinal or urogenital cancers.[14,15] Additionally, further studies are necessary to evaluate potential drug-drug interaction (DDI) between DOACs and commonly used cancer therapies.

DOACs like rivaroxaban and apixaban are primarily metabolized by the enzyme CYP3A4 and are transported across cell membranes by P-glycoprotein (P-gp).[16] Consequently, the effectiveness of DOACs can be significantly affected by substances that inhibit or enhance the activities of CYP3A4 and P-gp. Palbociclib, a cancer therapy known to inhibit CYP3A4, has the potential to alter the pharmacokinetic and pharmacodynamic profiles of rivaroxaban and apixaban.

Previous studies have shown that co-administration of strong CYP3A4 and P-gp inhibitors, such as ketoconazole, can substantially increase the exposure of DOACs, with the area under the curve (AUC) rising by 1.8 to 2.6 times, thereby heightening the risk of adverse events, including bleeding.[16] Similarly, research investigating the pharmacokinetic interactions between almonertinib, a P-gp and BCRP inhibitor, and DOACs (rivaroxaban and apixaban) in rats revealed a significant increase in systemic exposure to these anticoagulants.[17] Specifically, almonertinib increased the maximum concentration (C_{max}) and AUC of rivaroxaban by 3.3- and 3.6-fold, respectively, and apixaban by 2.69- and 2.87-fold. Additionally, the study indicated that almonertinib reduced the expression of Cyp3a1 in the liver and Abcb1a and Abcg2 in the intestine and kidney, further elucidating the mechanism of interaction.

Despite these insights, data regarding the specific interaction between palbociclib, another CYP3A4 and P-gp inhibitor, and DOACs such as rivaroxaban and apixaban remain limited. Palbociclib is an oral CDK4/6 inhibitor used mainly for advanced breast cancer that can alter the pharmacokinetics of other drugs by inhibiting CYP3A4 and drug transporters like P-gp and BCRP. Given the pharmacokinetic characteristics of palbociclib, similar interactions are anticipated, which could lead to increased drug exposure and associated bleeding risks.[18] Moreover, cancer patients are particularly susceptible to DDI involving DOACs, as they often take multiple medications as part of their cancer treatment or for managing comorbidities. Therefore, it is imperative to investigate these interactions in greater detail to inform dose adjustments and ensure the safe co-administration of these medications.

The objective of this study is to investigate the potential DDI between palbociclib and the direct oral anticoagulants rivaroxaban and apixaban. To achieve this, male Sprague-Dawley rats were divided into distinct treatment groups, receiving either palbociclib alone or in combination with apixaban or rivaroxaban. Blood samples were collected at various time points, and the plasma concentrations of the drugs were quantified using ultra-performance liquid chromatography-tandem mass spectrometry (UPLC-MS/MS). Additionally, quantitative real-time PCR (qRT-PCR) was performed on liver and intestinal tissues to evaluate the gene expression of key enzymes, including Cyp3a1 (the functional homolog of human CYP3A4), Abcb1a (the functional homolog of human P-gp) and Abcg2 (the functional homolog of human BCRP), involved in drug metabolism. Pharmacokinetic parameters were subsequently calculated, and statistical analyses were conducted to assess the significance of the observed drug interactions. The materials utilized, experimental procedures, and validation methods were meticulously applied to ensure the accuracy and reliability of the data.

Materials and Methods

Study Design and Treatments

Animals

Adult male Sprague-Dawley (SD) rats, specific pathogen-free (SPF), weighing 230 ± 30 g, were procured from Beijing Huafukang Biotechnology Co., Ltd. (Beijing, China; License No. SCXK (Jing) 2019–0008). All experimental protocols were approved by the Animal Ethics Committee of Hebei General Hospital (Shijiazhuang, China) (Approval No. 2024-DW-072). The rats were housed under controlled conditions (23 ± 2 °C, 12-hour light/dark cycle, 50 ± 10% relative humidity) and acclimatized for one week to ensure their health and minimize stress. Water was provided ad libitum, and food was withheld for 12 hours prior to drug administration.

Pharmacokinetic Study in Rats

The experimental rats were randomly assigned to 11 treatment groups (n = 6 per group) as detailed in Table 1. Group I, V and IX were vehicle controls to establish baseline parameters; Group II, VI, X and XI were designed to investigate DDI. Group III, IV, VII and VIII were structured to systematically assess dose modification approaches, including interval administration and dose reduction, to identify optimal coadministration strategies. Animals were randomly allocated using Microsoft Excel 365 (version 2308) RAND function with stratification. Doses were determined using the body surface area normalization method.[19] Palbociclib was suspended in methyl cellulose (MC), rivaroxaban in hydroxypropyl methyl cellulose (HPMC), and apixaban in a solution containing 5% dimethyl sulfoxide (DMSO). To achieve steady-state blood levels, palbociclib was administered orally by gavage for 8 consecutive days, while rivaroxaban and apixaban were administered orally by gavage for 5 consecutive days, corresponding to 5 to 7 half-lives needed for steady-state concentrations in vivo.

Table 1 Study Design

Study Design	Group No.	Treatment Description
Influence of Palbociclib on the Apixaban Pharmacokinetics		
Apixaban 0.5mg/kg alone	Group I	Apixaban 0.5mg/kg alone
Palbociclib + Apixaban	Group II	Palbociclib 11 mg/kg for 8 consecutive days + Apixaban 0.5mg/kg coadministered on the 8th day
Palbociclib + Apixaban (12h interval)	Group III	Palbociclib 11 mg/kg for 8 consecutive days + Apixaban 0.5mg/kg 12h after the final palbociclib administration on the 8th day
Palbociclib + Reduced Apixaban	Group IV	Palbociclib 11 mg/kg for 8 consecutive days + Apixaban 0.25mg/kg coadministered on the 8th day
Influence of Palbociclib on the Rivaroxaban Pharmacokinetics		
Rivaroxaban 2mg/kg alone	Group V	Rivaroxaban 2mg/kg alone
Palbociclib + Rivaroxaban	Group VI	Palbociclib 11 mg/kg for 8 consecutive days + Rivaroxaban 2mg/kg coadministered on the 8th day
Palbociclib + Rivaroxaban (12h interval)	Group VII	Palbociclib 11 mg/kg for 8 consecutive days + Rivaroxaban 2mg/kg 12h after the final palbociclib administration on the 8th day
Palbociclib + Reduced Rivaroxaban	Group VIII	Palbociclib 11 mg/kg for 8 consecutive days+ Rivaroxaban 1mg/kg coadministered on the 8th day
Influence of Rivaroxaban or Apixaban on the Palbociclib Pharmacokinetics		
Palbociclib 11 mg/kg alone	Group IX	Palbociclib 11 mg/kg alone
Apixaban + Palbociclib	Group X	Apixaban 0.5mg/kg for 5 consecutive days + Palbociclib 11 mg/kg coadministered on the 5th day
Rivaroxaban + Palbociclib	Group XI	Rivaroxaban 2mg/kg for 5 consecutive days + Palbociclib 11 mg/kg coadministered on the 5th day

Blood Sample and Tissue Collection

Blood samples (approximately 100 μL each) were collected into heparinized tubes at designated time points: 0, 0.25, 0.5, 1, 2, 4, 5, 6, 8, 10, 12, 24, and 48 hours for palbociclib; 0, 0.08, 0.17, 0.25, 0.34, 0.5, 0.75, 1, 3, 5, 7, 10, and 12 hours for apixaban; and 0, 0.17, 0.34, 0.5, 0.75, 1, 1.5, 2, 3, 4, 5, 6, 8, 10, and 12 hours for rivaroxaban. Sampling time points were determined based on FDA pharmacokinetic sampling guidelines and each drug's pharmacokinetic profile.[20] Blood samples were centrifuged at 3500 rpm for 10 minutes, and the plasma was collected and stored at −80 °C until analysis via ultra-performance liquid chromatography-tandem mass spectrometry (UPLC-MS/MS).

In this study, blank controls received daily oral gavage of MC solution (vehicle) for 8 consecutive days, matching the volume and schedule of palbocicilb-treated groups. On the eigth day post-treatment, liver and intestinal tissues were harvested for molecular analysis. Tissues were immediately stored at −80 °C until further processing.

UPLC-MS/MS Assay

Materials

Palbociclib (purity >98%, Lot 24W003-J5) was supplied by Shanghai Zhen Zhun Biotechnology Co., Ltd. (Shanghai, China). Palbociclib-d_8 (purity ≥99%, Lot C16350009) and apixaban (purity ≥98%, Lot C15069980) were obtained from Shanghai Macklin Bio-Technology Co., Ltd. (Shanghai, China). Rivaroxaban (purity ≥99%, Lot H25J9Z64216) was provided by Shanghai Yuan Ye Bio-Technology Co., Ltd. (Shanghai, China). Rivaroxaban-d4 (purity >98%, Lot 21,702) was sourced from B1203 Life Science Park, SCT Creative Factory (Shenzhen, China).

Dimethyl sulfoxide (DMSO) was purchased from Beijing Solarbio Science Technology Co., Ltd. (Beijing, China). High-performance liquid chromatography (HPLC)-grade acetonitrile, methyl tert-butyl ether, formic acid, and ammonium acetate were obtained from Fisher Scientific (Pittsburgh, PA, USA). Ultrapure water was acquired from Wahaha Group Co., Ltd. (Hangzhou, China).

Instruments and Analytical Conditions

Plasma concentrations of rivaroxaban and apixaban were determined using a previously established UPLC-MS/MS method.[17] Palbociclib was quantified using an LC-30A ultra-performance liquid chromatograph (Shimadzu, Japan) coupled with a Sciex Triple Quad 5500 tandem mass spectrometer (Sciex, USA). Chromatographic separation was performed on an XSelect HSS T3 column (2.1 mm × 100 mm, 2.5 μm) maintained at 40 °C during gradient elution. The mobile phase consisted of water (Phase A) and acetonitrile containing 0.1% formic acid (Phase B). The flow rate was set at 0.3 mL/min, and the gradient elution procedure was as follows: 0–2.5 minutes, 60% B; 2.5–3.5 minutes, 60–90% B; 3.5–5.5 minutes, 90% B; 5.5–5.6 minutes, 90–60% B; 5.6–6.6 minutes, 60% B. The injection volume was 1 μL.

Preparation of Calibration Standards and Quality Control (QC) Samples

Palbociclib (1 mg/mL) and internal standards (IS, 1 mg/mL) were prepared by dissolving in dimethyl sulfoxide (DMSO). Working solutions for calibration were obtained by diluting the stock solutions with a 50% acetonitrile-water mixture to achieve final concentrations of 1, 5, 10, 50, 200, 500, 1000, and 2000 ng/mL. Calibration standards were prepared by spiking 5 μL of the working solution into 45 μL of blank rat plasma. Quality control (QC) samples at concentrations of 2, 400, and 1500 ng/mL were prepared similarly. All stock solutions, working solutions, calibration standards, and QC samples were stored at −20 °C until analysis.

Method Validation

The analytical method was validated in accordance with the FDA's M10 Bioanalytical Method Validation guidelines.[21] Selectivity was evaluated using blank plasma samples from six different rats, samples spiked with analytes at the lower limit of quantification (LLOQ) and internal standards (IS), and actual plasma samples post-palbociclib administration. The peak area of the blank plasma at the analyte retention time did not exceed 20% of the LLOQ and 5% of the IS, ensuring no significant interference from endogenous substances.

Calibration curves were constructed by spiking standard solutions into blank plasma across a concentration range of 1–2000 ng/mL as described in Preparation of Calibration Standards and Quality Control (QC) Samples. The LLOQ acceptance limit was within ±20% of the nominal value, and all other calibration levels were within ±15%. Accuracy and

precision were determined using six replicates of the LLOQ and QC samples at three different concentrations, evaluated on a single day and over three consecutive days. The relative standard deviation (RSD) for intra- and inter-day precision and the relative error (RE) remained within ±15% of the nominal concentration, and within ±20% for the LLOQ. Recovery and matrix effects were assessed by analyzing three levels of QC samples (n = 6). Stability studies were conducted at low and high QC concentrations under four conditions: room temperature (25 °C) for 8 hours, autosampler temperature (15 °C) for 8 hours, −80 °C for 7 days, and after three freeze-thaw cycles (−80 °C to 25 °C).

Pharmacokinetic Assessment and Analysis

Determination of Plasma Concentrations

To determine plasma concentrations, 2.5 μL of the internal standard (IS) working solution was added to 25 μL of the plasma sample, followed by 150 μL of acetonitrile. The mixture was vortexed for 1 minute and centrifuged at 12,000 rpm for 10 minutes. Subsequently, 70 μL of the supernatant was combined with 70 μL of 50% acetonitrile-water and briefly vortexed for an additional 1 minute. Finally, 1 μL of the resulting solution was injected into the UPLC-MS/MS for analysis.

Pharmacokinetic Evaluation

Pharmacokinetic parameters in rats were evaluated and calculated using a noncompartmental model with DAS 2.1.1 Software (Mathematical Pharmacology Professional Committee of China, Shanghai, China) for rivaroxaban, apixaban, and palbociclib. Parameters calculated included elimination half-life (t1/2), maximum plasma concentration (C_{max}), time to reach C_{max} (T_{max}), total area under the concentration-time curve ($AUC_{0\text{-}t}$ and $AUC_{0\text{-}\infty}$), clearance of drug plasma volume per time unit ($CL_{z/F}$), apparent volume of distribution ($V_{z/F}$), and mean residence time ($MRT_{0\text{-}t}$, $MRT_{0\text{-}\infty}$).

Quantitative Real-Time PCR Analysis

Frozen liver and intestinal tissues from rats were processed using the TRNzol extraction method to isolate total RNA, following the manufacturer's guidelines. A 2 μL aliquot of the total RNA solution was analyzed using a Bio Tek Epoch spectrophotometer (Bio Tek Instruments, Inc., Winooski, VT, USA) to determine RNA concentration and purity, as assessed by the 260/280 nm absorbance ratio. One microgram of RNA was converted to complementary DNA (cDNA) using the FastKing RT Kit. The reaction mixture for the multiplex qRT-PCR contained 10 μL of 2 × SuperReal PreMix Plus, 0.4 μL of ROX Reference Dye, 0.6 μL of each primer, and RNase-free ddH_2O to achieve a final volume of 20 μL. The PCR conditions were as follows: denaturation at 95°C for 15 minutes, followed by 40 cycles of 95°C for 10 seconds and 60°C for 32 seconds. Optimal conditions were determined to achieve the maximum ΔRn and the minimum cycle threshold (Ct) value. Each sample was analyzed in triplicate for this experiment, with NADPH serving as an internal reference for normalization. The SLAN-96S Real-time PCR system (Shanghai Hongshi Medical Technology Co., Ltd., Shanghai, China) was employed for PCR assays. The tissue samples of the blank control were also treated to establish the baseline gene expression level (qPCR analysis was set to 1.0). Data were analyzed using the $2^{-\Delta\Delta CT}$ method, and statistical analyses of the experimental data were conducted using SPSS. The PCR primer sequences used for amplification are listed in Table 2.

Statistical Analysis

The sample size (n = 6 per group) was determined using the resource equation method.[22] For one-way analysis of variance (ANOVA), the minimum sample size was calculated as n = 10/ (k + 1), where k represents the number of groups.

Table 2 Primer Sequences Used in qRT-PCR

Gene	Forward Primer	Reverse Primer
Cyp3a1	5'-TGCATTGGCATGAGGTTTGC-3'	5'-TTCAGCAGAACTCCTTGAGGG-3'
Abcb1a	5'-TCTGGTATGGGACTTCCTTGGT-3'	5'-TCCTTGTATGTTGTCGGGTTTG-3'
Abcg2	5'-TGAAGAGTGGCTTTCTAGTCCG-3'	5'-TTGAAATTGGCAGGTTGAGGTG-3'
NADPH	5'-GCCTTCCGTGTTCCTACC-3'	5'-GCCTGCTTCACCACCTTC-3'

https://doi.org/10.2147/DDDT.S499209

In this study, comparing pharmacokinetic parameters between two treatment groups (experimental and control) resulted in a sample size per group of $n = 10/2 + 1 = 6$.

Pharmacokinetic variables were expressed as geometric mean values with standard deviations. Statistical analyses were performed using SPSS software (SPSS Inc., Chicago, IL, USA). For comparisons between two groups, normality was verified using the Shapiro–Wilk test, supplemented by visual inspection of Q-Q plots due to the small sample size ($n = 6$ per group). Levene's test was conducted to assess the homogeneity of variances between groups, with a significance threshold set at $p < 0.05$. When variances were equal ($p > 0.05$), two-tailed t-tests were applied. When variances were unequal ($p < 0.05$), the Satterthwaite correction was utilized. Differences between parameters that deviated significantly from normality were assessed using the Mann–Whitney *U*-test (two-tailed).

Data normality was assessed using the Shapiro–Wilk test, with visual verification via Q-Q plots. Homogeneity of variances was examined using Levene's test. For group comparisons where data met both normality and homogeneity of variance assumptions, one-way ANOVA was conducted, followed by Bonferroni post hoc tests to control for Type I error. If Levene's test indicated significant heterogeneity of variances ($p < 0.05$), Welch's ANOVA was applied with Games-Howell post hoc comparisons. For repeated measurements from the same subjects, repeated-measures ANOVA was used; if Mauchly's test indicated sphericity violation, the Greenhouse-Geisser correction was applied. Significant ANOVA results were followed by Bonferroni-corrected pairwise comparisons. For repeated measures data violating normality or homogeneity assumptions, the non-parametric Friedman test was used, with Nemenyi post hoc tests for significant results. For non-repeated measures data violating assumptions, the Kruska-Wallis test with appropriate post hoc comparisons was employed.

Results

Method Development and Validation

A highly sensitive and reproducible UPLC-MS/MS method was developed to evaluate the plasma concentration of palbociclib in rats. Various liquid chromatographic conditions, including column type and mobile phase composition, were optimized to achieve optimal peak symmetry, high detection sensitivity, and reduced retention times. An XSelect HSS T3 column (2.1 mm × 100 mm, 2.5 μm) was maintained at 40 °C, facilitating adequate separation of the analytes and the internal standard (IS). The addition of formic acid to the organic phase B enhanced the chromatographic signals and peak profiles of palbociclib, demonstrating superior elution capacity compared to methanol. A gradient elution procedure was employed, starting with an initial acetonitrile ratio of 40% at a flow rate of 0.3 mL/min, resulting in high detection sensitivity and shortened retention times. Mass spectrometry for all analytes was conducted in positive mode using multiple reaction monitoring (MRM), with ion transitions yielding the highest responses at m/z 448.3→380.2 for palbociclib and 456.3→388.3 for the IS (Figure 1). Additional details regarding the optimization of mass parameter conditions are summarized in Table 3.

The calibration curve for palbociclib was linear within the range of 1–2000 ng/mL ($r = 0.999$). Precision values for palbociclib at three quality control concentrations and the lower limit of quantification (LLOQ) did not exceed

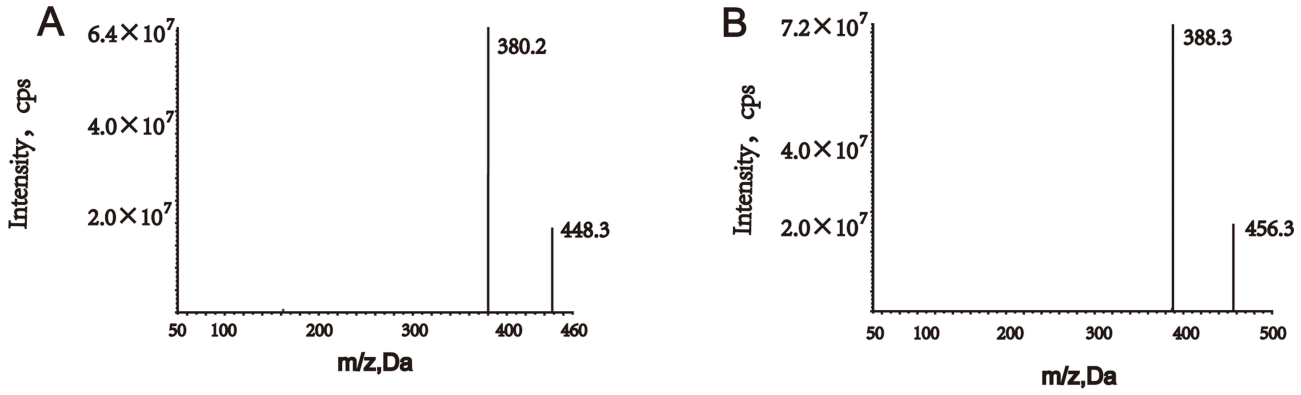

Figure 1 Product ion mass spectrum of palbociclib (**A**) and palbociclib-d_8 (**B**).

Table 3 Experimental Settings for the Tandem Mass-Spectrometer for the Analytes and Internal Standards

Experimental Setting	Palbociclib	Palbociclib-d_8
MRM transition	448.3→380.2	456.3→388.3
Delustering potential (DP), V	130	130
Collision energy (CE), V	35	35
Collision cells exit potential (CXP), V	14	14
Entrance potential (EP), V	10	10

7.58%, while accuracy ranged from −4.75% to 6.58%. Matrix effects were less than 109.57%, indicating no significant matrix effect in rat plasma. Recovery rates, normalized by the IS peak area from the plasma matrix, ranged from 99.41% to 107.44% (RSD < 14%). Stability studies demonstrated that under all four storage and handling conditions (room temperature, 15 °C in the autosampler, −80 °C, and after three freeze-thaw cycles), the relative error (RE) was less than 7% and the relative standard deviation (RSD) was less than 10%, indicating excellent stability of the samples using the specified preparation, storage, and measurement methods.

Pharmacokinetic Interactions

Effect of Palbociclib on the Pharmacokinetics of Apixaban

The plasma concentration-time profiles of apixaban administered at doses of 0.5 mg/kg or 0.25 mg/kg, either alone or in conjunction with simultaneous and delayed administration of palbociclib, are shown in Figure 2. The main

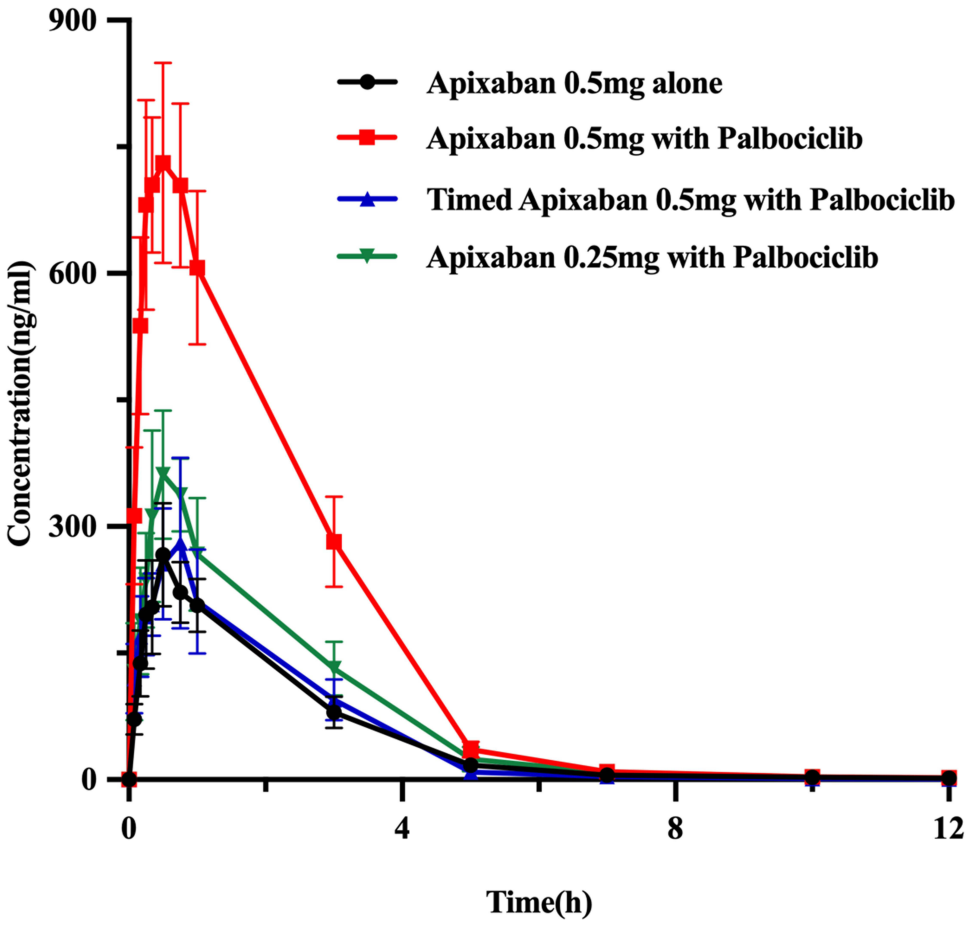

Figure 2 Mean plasma concentration-time profiles of apixaban after oral administration alone and following multiple doses and timed of palbociclib.

https://doi.org/10.2147/DDDT.S499209

pharmacokinetic parameters of apixaban, obtained using non-compartmental methods, are summarized in Table 4. (Apixaban 0.25 mg/kg alone was shown in Table S1 and Figure S1). With simultaneous administration of palbociclib, the maximum plasma concentration C_{max}, area under the concentration-time curve from time zero to the last measurable concentration $AUC_{0\text{-}t}$, and area under the concentration-time curve from time zero to infinity $AUC_{0\text{-}\infty}$ of apixaban (0.5 mg/kg) significantly increased by 243.61% (p = 0.003, 95%Cl [−1045, −276]), 258.36% (p = 0.011, 95%Cl [−2747, −453]), and 256.64% (p = 0.012, 95%Cl [−2753, −448]), respectively, compared to the apixaban-only group. The clearance $CL_{z/F}$ and apparent volume of distribution $V_{z/F}$ of apixaban decreased by 72.53% (p = 0.013, 95%Cl [0.18, 1.15]) and 73.73% (p = 0.012, 95%Cl [0.31, 3.17]), respectively, compared to the control group.

When apixaban was administered at a dose of 0.25 mg/kg alongside palbociclib, the $AUC_{0\text{-}t}$, $AUC_{0\text{-}\infty}$, and C_{max} of apixaban showed slight increases of 43.35%, 43.49%, and 45.03%, respectively, although no statistical significance was observed. There were no significant differences for $CL_{z/F}$, T_{max}, half-life ($t_{1/2}$), $V_{z/F}$, mean residence time from time zero to the last measurable concentration $MRT_{0\text{-}t}$, and mean residence time from time zero to infinity $MRT_{0\text{-}\infty}$. However, when palbociclib was administered 12 hours later, the pharmacokinetic parameters of apixaban were not affected.

Effect of Palbociclib on the Pharmacokinetics of Rivaroxaban

The mean plasma concentration-time curves of rivaroxaban administered at doses of 2 mg/kg or 1 mg/kg, either alone or in conjunction with simultaneous and delayed administration of palbociclib, are presented in Figure 3. The main pharmacokinetic parameters of rivaroxaban are displayed in Table 5. (Rivaroxaban 1 mg/kg alone was shown in Table S2 and Figure S2). When rivaroxaban was co-administered simultaneously with palbociclib, the area under the concentration-time curve from time zero to the last measurable concentration $AUC_{0\text{-}t}$, area under the concentration-time curve from time zero to infinity $AUC_{0\text{-}\infty}$, and maximum plasma concentration C_{max} significantly increased by 380.77% (p < 0.001, 95%Cl [−3252, −2066]), 386.17% (p < 0.001, 95%Cl [−3175, −2467]), and 375.21% (p = 0.003, 95%Cl [−804, −265]), respectively. The clearance $CL_{z/F}$ and apparent volume of distribution $V_{z/F}$ of rivaroxaban were significantly decreased by 80.00% (p < 0.001, 95%Cl [0.34, 0.77]) and 75.86% (p = 0.035, 95%Cl [0.16, 3.36]), respectively, compared to the control group. Additionally, no significant differences were observed for T_{max}, half-life ($t_{1/2}$), mean residence time from time zero to the last measurable concentration $MRT_{0\text{-}t}$, and mean residence time from time zero to infinity $MRT_{0\text{-}\infty}$.

When comparing rivaroxaban at a dose of 2 mg/kg, multiple doses of palbociclib significantly increased the $AUC_{0\text{-}t}$, $AUC_{0\text{-}\infty}$, and C_{max} of rivaroxaban at 1 mg/kg by 161.86% (p < 0.001, 95%Cl [−1469, −791]), 150.93% (p < 0.001, 95% Cl [−1456, −748]), and 243.63% (p < 0.001, 95%Cl [−408, −285]), respectively. The $MRT_{0\text{-}t}$ and $MRT_{0\text{-}\infty}$ were significantly decreased by 27.82% (p = 0.006, 95%Cl [0.32, 1.79]) and 35.43% (p = 0.014, 95%Cl [0.25, 2.86]), respectively. The clearance $CL_{z/F}$ and apparent volume of distribution $V_{z/F}$ of rivaroxaban were significantly decreased by 60.87% (p = 0.002, 95%Cl [0.22, 0.63]) and 77.46% (p = 0.031, 95%Cl [0.22, 3.44]), respectively. There were no

Table 4 Pharmacokinetic Parameters of Apixaban in Rats When Administered Alone and Following Simultaneous and Timed Administration of Palbociclib

Parameters (Unit)	Apixaban 0.5 mg/kg			Apixaban 0.25mg/kg + Palbociclib
	Alone	+ Palbociclib	+ Timed Palbociclib (12 h)	
$AUC_{0\text{-}t}$ (μg/L*h)	578.78(GSD 1.49) (110.1%)	2109.09(GSD 1.42) (101.3%)*	635.36(GSD 1.23) (72.3%)	882.94(GSD 1.12) (51.4%)
$AUC_{0\text{-}\infty}$ (μg/L*h)	582.57(GSD 1.49) (110.4%)	2113.29(GSD 1.42) (101.3%)*	637.26(GSD 1.23) (72.2%)	890.39(GSD 1.12) (50.4%)
C_{max} (μg/L)	242.89(GSD 1.68) (135.3%)	900.99(GSD 1.34) (89.1%)**	277.93(GSD 1.35) (90.8%)	391.21(GSD 1.12) (51.3%)
T_{max} (h)	0.53(GSD 1.60) (124.6%)	0.48(GSD 1.76) (144.6%)	0.55(GSD 1.81) (151.3%)	0.56(GSD 1.46) (106.0%)
$t_{1/2}$ (h)	1.80(GSD 1.30) (82.5%)	1.77(GSD 1.29) (81.2%)	1.90(GSD 1.20) (66.8%)	2.29(GSD 1.68) (134.5%)
CL_z (L/h/kg)	0.86(GSD 1.49) (110.3%)	0.24(GSD 1.42) (101.2%)*	0.78(GSD 1.23) (72.2%)	0.56(GSD 1.12) (50.3%)
V_z (L/kg)	2.23(GSD 1.48) (108.7%)	0.60(GSD 1.29) (81.2%)*	2.15(GSD 1.32) (86.7%)	1.85(GSD 1.71) (139.0%)
$MRT_{0\text{-}t}$ (h)	1.83(GSD 1.24) (73.8%)	1.74(GSD 1.13) (53.5%)	1.71(GSD 1.12) (50.5%)	1.91(GSD 1.23) (71.5%)
$MRT_{0\text{-}\infty}$ (h)	1.92(GSD 1.25) (74.5%)	1.77(GSD 1.14) (54.6%)	1.74(GSD 1.13) (52.2%)	2.03(GSD 1.25) (74.9%)

Notes: *P<0.05, **P<0.01, compared to apixaban alone. Pharmacokinetic parameters are expressed as the geometric mean ± geometric standard deviation (geometric CV%).

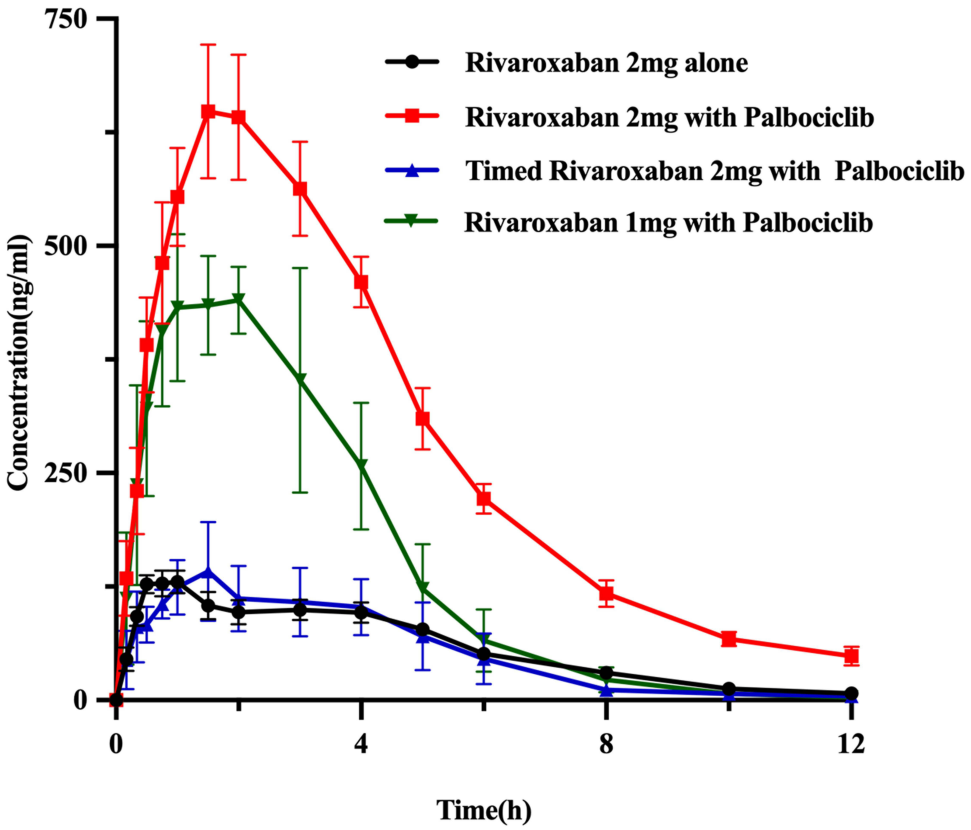

Figure 3 Mean plasma concentration-time profiles of rivaroxaban after oral administration alone and following multiple doses and timed of palbociclib.

significant differences for T_{max} and $t_{1/2}$. However, when palbociclib was administered 12 hours later, the pharmacokinetic parameters of rivaroxaban were not affected.

Effect of Rivaroxaban or Apixaban on the Pharmacokinetics of Palbociclib

The plasma concentration-time profile of palbociclib, administered alone or following multiple doses of rivaroxaban or apixaban, is presented in Figure 4, and the pharmacokinetic parameters are summarized in Table 6. When palbociclib and apixaban were co-administered, the area under the concentration-time curve from time zero to the last measurable concentration AUC_{0-t}, area under the concentration-time curve from time zero to infinity $AUC_{0-\infty}$, and maximum plasma

Table 5 Pharmacokinetic Parameters of Rivaroxaban in Rats When Administered Alone and Following Simultaneous and Timed Administration Palbociclib

Parameters (Unit)	Rivaxaban 2mg/kg			Rivaxaban 1mg/kg + Palbociclib
	Alone	+ Palbociclib	+ Timed Palbociclib (12 h)	
AUC_{0-t} (μg/L*h)	690.91(GSD 1.18) (62.8%)	3337.73(GSD 1.13) (52.5%)**	639.4(GSD 1.28) (79.7%)	1816.72(GSD 1.14) (54.2%)**
$AUC_{0-\infty}$ (μg/L*h)	721.62(GSD 1.20) (65.6%)	3541.98(GSD 1.09) (42.5%)**	654.28(GSD 1.26) (76.5%)	1820.98(GSD 1.14) (54.3%)**
C_{max} (μg/L)	140.50(GSD 1.21) (67.7%)	658.34(GSD 1.29) (82.1%)**	169.15(GSD 1.27) (77.5%)	488.35(GSD 1.08) (41.5%)**
T_{max} (h)	1.02(GSD 2.05) (178.6%)	1.94(GSD 1.29) (81.6%)	1.47(GSD 1.63) (129.2%)	1.54(GSD 1.52) (115.0%)
$t_{1/2}$ (h)	2.13(GSD 1.68) (135.5%)	2.60(GSD 1.34) (89.2%)	2.00(GSD 1.98) (170.8%)	1.22(GSD 1.10) (45.4%)
CL_z (L/h/kg)	0.69(GSD 1.20) (65.6%)	0.14(GSD 1.09) (42.4%)**	0.76(GSD 1.26) (76.4%)	0.27(GSD 1.14) (54.5%)**
V_z (L/kg)	2.13(GSD 1.55) (118.4%)	0.53(GSD 1.42) (100.5%)*	2.21(GSD 2.30) (207.2%)	0.48(GSD 1.19) (63.7%)*
MRT_{0-t} (h)	3.81(GSD 1.12) (49.9%)	3.79(GSD 1.10) (46.8%)	3.32(GSD 1.13) (51.6%)	2.75(GSD 1.17) (60.1%)**
$MRT_{0-\infty}$ (h)	4.29(GSD 1.21) (67.2%)	4.45(GSD 1.22) (70.6%)	3.67(GSD 1.07) (38.4%)	2.77(GSD 1.17) (61.2%)*

Notes: *P<0.05, **P<0.01, compared to rivaroxaban alone. Pharmacokinetic parameters are expressed as the geometric mean ± geometric standard deviation (geometric CV%).

https://doi.org/10.2147/DDDT.S499209

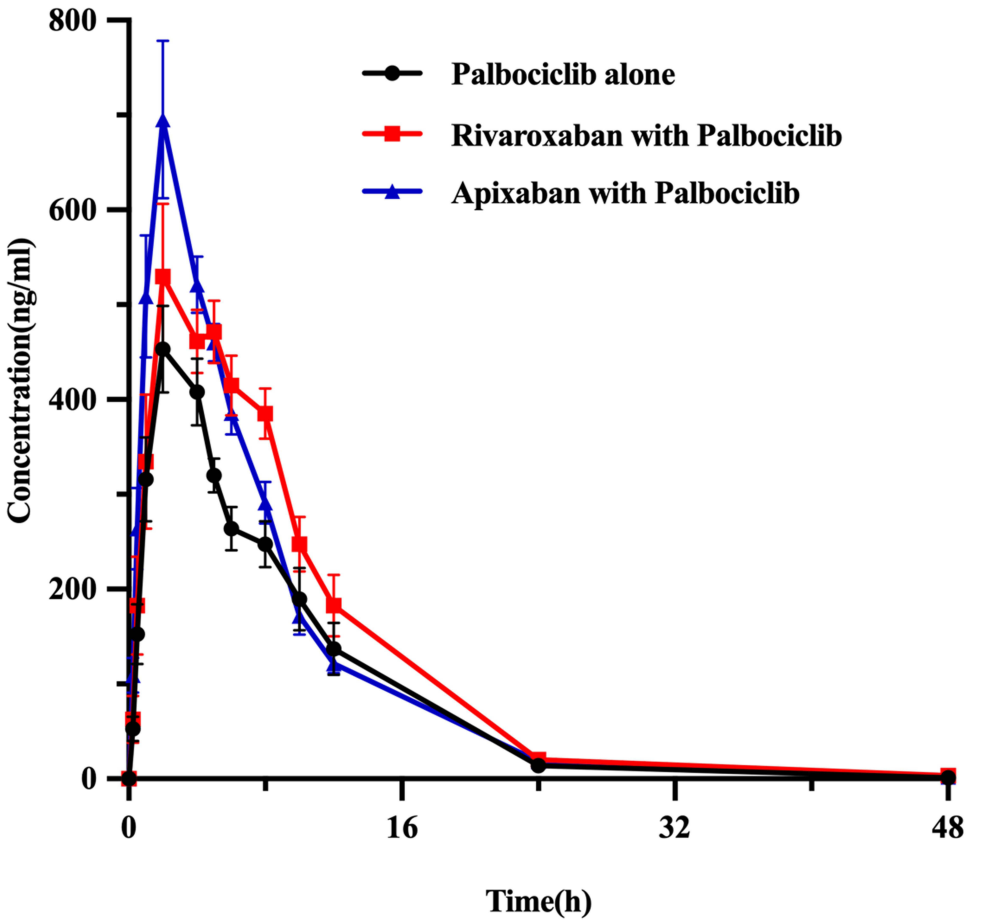

Figure 4 Mean plasma concentration-time profiles of palbociclib after oral administration alone and following multiple doses of rivaroxaban or apixaban.

concentration C_{max} of palbociclib increased by 24.75% (p = 0.042, 95%Cl [−2134, −49]), 24.83% (p = 0.042, 95%Cl [−2147, −47]), and 49.30% (p = 0.015, 95%Cl [−414, −58]), respectively. No statistically significant changes were observed for other pharmacokinetic parameters between the groups. Coadministration of palbociclib with rivaroxaban resulted in an increase in the $AUC_{0\text{-}t}$ and $AUC_{0\text{–}\infty}$ levels of palbociclib by 32.94% (p = 0.02, 95%Cl [−2625, −280]) and 33.13% (p = 0.02, 95%Cl [−2647, −282]) without any notable change in other PK parameters.

Table 6 Pharmacokinetic Parameters of Palbociclib in Rats When Administered Alone and Following Rivaroxaban or Apixaban

Parameters (Unit)	Palbociclib		
	Alone	+ Apixaban	+ Rivaroxaban
$AUC_{0\text{-}t}$ (μg/L*h)	4340.45(GSD 1.22) (70.2%)	5459.93(GSD 1.15) (56.9%)*	5797.19(GSD 1.19) (63.7%)*
$AUC_{0\text{-}\infty}$ (μg/L*h)	4347.69(GSD 1.22) (70.5%)	5518.34(GSD 1.15) (57.0%)*	58,815.97(GSD 1.19) (64.0%)*
C_{max} (μg/L)	469.12(GSD 1.25) (75.4%)	698.52(GSD 1.27) (79.0%)*	563.47(GSD 1.29) (81.7%)
T_{max} (h)	2.83(GSD 1.46) (106.6%)	2.24(GSD 1.33) (87.2%)	2.94(GSD 1.85) (155.1%)
$t_{1/2}$ (h)	3.99(GSD 1.44) (104.1%)	5.41(GSD 1.30) (83.8%)	5.09(GSD 1.33) (87.1%)
CL_z (L/h/kg)	0.01(GSD 1.25) (74.8%)	0.01(GSD 1.00) (0.0%)	0.01(GSD 1.00) (0.0%)
V_z (L/kg)	0.01(GSD 1.36) (92.4%)	0.02(GSD 1.27) (79.0%)	0.01(GSD 1.26) (76.8%)
$MRT_{0\text{-}t}$ (h)	7.33(GSD 1.25) (74.5%)	7.02(GSD 1.15) (57.0%)	8.07(GSD 1.13) (51.7%)
$MRT_{0\text{-}\infty}$ (h)	7.39(GSD 1.26) (76.4%)	7.15(GSD 1.15) (56.5%)	8.24(GSD 1.11) (48.3%)

Notes: *p<0.05, compared to palbociclib alone. Pharmacokinetic parameters are expressed as the geometric mean ± geometric standard deviation (geometric CV%).

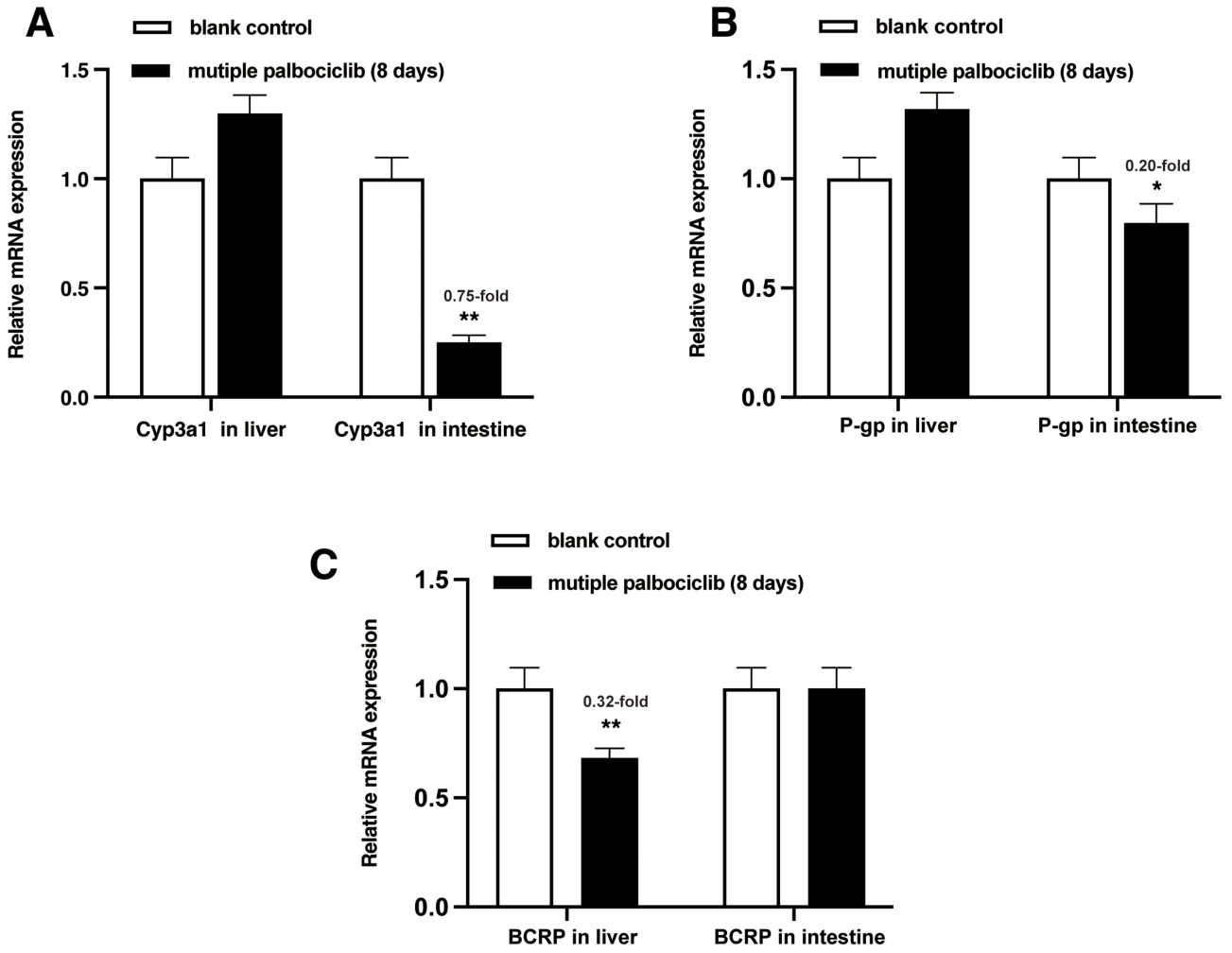

Figure 5 Relative mRNA expression in liver and intestine. (**A**) Effect of multiple-doses palbociclib administration on mRNA expression of Cyp3a1 in liver and intestine; (**B**) Effect of multiple-doses palbociclib administration on mRNA expression of P-gp in liver and intestine; (**C**) Effect of multiple-doses palbociclib administration on mRNA expression of BCRP in liver and intestine. *p < 0.05, **p < 0.01.

Messenger RNA (mRNA) Expression in Rat Liver and Intestines

The relative mRNA expression levels in the liver and intestines of the rats are presented in Figure 5. After the administration of palbociclib for eight consecutive days, the mRNA expression of Cyp3a1 and P-gp in the intestine was downregulated by 74.97% ($p < 0.001$) and 20.17% ($p = 0.016$), respectively; however, there was no significant effect on the expression of Cyp3a1 and P-gp in the liver (Figure 5A and B). Additionally, the effect of palbociclib on the mRNA expression of BCRP in the liver decreased by 31.66% ($p = 0.006$), while no significant inhibition was observed in the intestine (Figure 5C).

Discussion

This study reveals a significant pharmacokinetic interaction between palbociclib and the DOACs apixaban and rivaroxaban, characterized by a marked increase in drug exposure. Co-administration of palbociclib resulted in a 2.1- to 2.5-fold increase in the area under the concentration-time curve (AUC) and maximum plasma concentration C_{max} of apixaban, and a 4- to 5-fold increase in AUC and C_{max} of rivaroxaban compared to controls. PCR results suggest that palbociclib likely enhances DOAC exposure primarily through increased intestinal absorption mediated by decreased P-gp and BCRP expression, indicating markedly improved bioavailability for both drugs. Importantly, these results highlight the potential for increased bleeding risk when these drugs are used concurrently, underscoring the necessity for careful dose

https://doi.org/10.2147/DDDT.S499209

adjustment and clinical monitoring. This study is among the first to investigate the interaction between palbociclib and direct oral anticoagulants, providing critical insights for managing cancer patients receiving both treatments.

Effects of Palbociclib on the Pharmacokinetics of Apixaban (0.5 and 0.25 mg/Kg) or Rivaroxaban (2 and 1 mg/Kg)

The co-administration of palbociclib resulted in a significant increase in exposure to apixaban. Compared to the control group, the palbociclib and apixaban (0.5 mg/kg) groups exhibited nearly a 2.1-fold increase in both the area under the concentration-time curve (AUC) and maximum plasma concentration C_{max} of apixaban. Similarly, a nearly 4-fold increase in AUC and C_{max}, along with decreases in clearance $CL_{z/F}$ and apparent volume of distribution $V_{z/F}$ of rivaroxaban (2 mg/kg), were observed in rats co-administered with palbociclib, suggesting an increase in the bioavailability of the drug.

CYP3A4 is the primary cytochrome P450 enzyme present in the intestines and liver, playing a crucial role in the metabolism of a diverse range of xenobiotic substances, including therapeutic medications.[23] When assessing the effects of CYP3A4 modulators, it is important to consider the functional relationship between the drug efflux transporter P-gp and CYP3A4. Certain drugs can affect both systems as inhibitors or inducers, and the combined impact of modulating P-gp and CYP3A4 may be more significant than the individual effects of modulating either pathway alone.[24] For example, diltiazem and ketoconazole, which are strong inhibitors of both CYP3A4 and P-gp, significantly affect the systemic exposure of apixaban.[25] Similarly, verapamil (a strong inhibitor of CYP3A4/P-gp) and diltiazem (a moderate inhibitor) significantly increased the systemic exposure of rivaroxaban.[26]

Multiple studies have indicated that palbociclib is both a substrate and modulator of P-gp and CYP3A4.[27] Therefore, we speculate that the increased exposure of DOACs in the presence of palbociclib can most likely be attributed to the enhancement of intestinal absorption. This is consistent with our PCR results, which demonstrated that palbociclib inhibits the expression of P-gp in the intestine, leading to increased bioavailability due to the inhibition of intestinal P-gp-mediated transport processes during the absorption phase of apixaban[25] or rivaroxaban.[26]

In addition to P-gp interactions, other transporters may have clinically significant effects on the absorption and disposition of apixaban and rivaroxaban. Compared to P-gp, breast cancer resistance protein (BCRP) exhibits a higher affinity, suggesting that the role of BCRP in DDI involving rivaroxaban and apixaban cannot be excluded. In vitro studies indicate that palbociclib, apixaban, and rivaroxaban are all substrates of BCRP, and PCR analysis demonstrated that palbociclib significantly downregulated hepatic BCRP mRNA expression in rats, which suggests a plausible mechanistic basis for the observed increased anticoagulant exposure in our study potentially through competitive inhibition of BCRP-mediated transport.[28]

Since apixaban and rivaroxaban are direct reversible inhibitors of factor Xa, the primary concern with increased exposure is the inherent risk of bleeding.[29,30] Therefore, to minimize or eliminate this drug-drug interaction and provide an appropriate dose adjustment strategy for clinical use, further studies were conducted. Initially, we chose to reduce the doses of rivaroxaban and apixaban by half to explore whether lower doses would mitigate the influence of palbociclib. However, we found that the C_{max} and AUC of apixaban increased by 2.1- and 2.2-fold, respectively, while the C_{max} and AUC of rivaroxaban increased by 4.4- and 4.6-fold. Thus, dose reduction was ineffective when apixaban was administered with inhibitors of CYP3A4 and/or P-gp.

Furthermore, we investigated the influence of dosing intervals in depth, administering palbociclib 12 hours prior to rivaroxaban or apixaban. Notably, after palbociclib administration for 12 hours, there were no changes in the pharmacokinetic parameters of apixaban or rivaroxaban. Based on the available evidence, we hypothesize that the observed DDIs primarily occur during the absorption phase. Palbociclib's inhibitory effect on intestinal transporters appears to be time-dependent and reversible, explaining why no significant interaction effects were observed when drugs were administered with a temporal separation. This design is clinically meaningful, as it simulates simultaneous and timed administration with a CYP3A4/P-gp inhibitor, potentially defining a safe dosing schedule for the clinical combination of apixaban or rivaroxaban with a potent CYP3A4/P-gp inhibitor.

Effects of Apixaban or Rivaroxaban on Palbociclib Pharmacokinetics

Co-administration of apixaban moderately increased the exposure to palbociclib by 24.75% (based on AUC) and by 49.30% (based on C_{max}), while rivaroxaban slightly increased palbociclib exposure by 32.94% (based on AUC). Since co-administration of apixaban or rivaroxaban did not alter t_{max} or $t_{1/2z}$ of palbociclib, it can be concluded that metabolism inhibition is not the primary reason for the increased exposure to palbociclib. This effect is presumably related to the action of efflux transporters P-gp and breast cancer resistance protein (BCRP). These findings are consistent with previous studies indicating that rivaroxaban increases the exposure of almonertinib, which is a substrate of CYP3A4 and P-gp.[17] P-gp mediates the export of drugs from cells located in the small intestine, blood-brain barrier, liver, and proximal renal tubules, providing a protective function against foreign substances. Consequently, the intestinal absorption, biliary excretion, and urinary excretion of P-gp substrates can be altered by the inhibition or induction of P-gp.[31]

As both palbociclib and apixaban or rivaroxaban are substrates of P-gp and BCRP, we hypothesize that the increased exposure to palbociclib may be attributed to competition for the same transport pathways. Therefore, the observed effects may primarily be explained by an increased fraction of palbociclib reaching systemic circulation due to decreased intestinal efflux transport. However, further studies are needed to explore the underlying mechanisms. Given the alterations in palbociclib exposure when taken with DOACs, healthcare providers should be vigilant regarding the potential for this DDI and monitor complete blood counts closely.

It is also crucial to address the limitations of this study. First, no experimental animal models for cancer or thromboembolism were established to evaluate the DDI. Given that cancer can impair hepatic and renal function—potentially downregulating CYPs and UGTs—this may alter drug pharmacokinetics and reduce clearance.[32,33] Therefore, co-administration of these drugs could lead to clinically significant pharmacokinetic DDIs.[34] Secondly, female rats undergo a 4–5-day estrous cycle, causing fluctuations in drug metabolism (eg, CYP450 enzyme activity varies by up to 40% across phases) and physiological responses. Therefore, male Sprague-Dawley rats were chosen to eliminate hormonal effects, and thus, the study did not compare findings by gender. Additionally, species-specific differences in drug metabolism, particularly in CYP3A-mediated pathways, limit the direct extrapolation of these findings to humans. Despite these constraints, the study provides valuable preliminary insights into potential DDIs involving investigational drugs, which can guide future clinical DDI research. Additional clinical studies are needed to determine optimal dose adjustments for concomitant use of these therapies.

Conclusion

In this study, we developed and validated a sensitive, rapid, reliable, and accurate UPLC-MS/MS method for quantifying palbociclib in rat plasma. The results demonstrated that multiple doses of palbociclib significantly enhanced systemic exposure to apixaban and rivaroxaban in rats. This increased exposure to DOACs, as a result of DDI, may elevate the risk of bleeding. Additionally, co-administration of apixaban or rivaroxaban slightly enhanced the oral bioavailability of palbociclib, with efflux transporters playing a crucial role in this process.

Our findings may inform a dosing schedule that helps adjust doses appropriately to avoid toxic effects in patients. Considering the dosing frequencies of these medications (palbociclib once daily, rivaroxaban once/twice daily and apixaban twice daily), it is recommended to administer the palbociclib and rivaroxaban12 hours apart when clinically feasible to minimize the DDI effect, and for rivaroxaban, dose at least 6h apart from palbociclib when 12h separation is impractical. However, the proposed adjustments to drug administration regimens remain hypothetical and are not yet evidence-based recommendations. Further clinical studies in humans will be necessary to validate these findings. If validated, real-world pharmacovigilance studies should assess adverse events in co-medicated patients, followed by dose-optimization trials to mitigate risks.

Data Sharing Statement

The data presented in this study are available on request from the corresponding author.

Ethical Statement

The authors are accountable for all aspects of the work in ensuring that questions related to the accuracy or integrity of any part of the work are appropriately investigated and resolved. The animal experiment protocol was approved by the Hebei General Hospital Ethics Committee (Shijiazhuang, Hebei, China). All experimental procedures were fulfilled based on the FDA Guide for the Care and Use of Laboratory Animals (USA 1985). We present the article in accordance with the ARRIVE reporting checklist.

Acknowledgments

We acknowledge the support of the Hebei General Hospital Clinical Research Center, Shijiazhuang, Hebei, China.

Funding

This research received no external funding.

Disclosure

The authors report no conflict of interest associated with this research work.

References

1. Lloyd AJ, Dewilde S, Noble S, Reimer E, Lee AYY. What impact does venous thromboembolism and bleeding have on cancer patients' quality of life? *Value Health*. 2018;21(4):449–455. doi:10.1016/j.jval.2017.09.015
2. Fernandes CJ, Morinaga LTK, Alves JLJ, et al. Cancer-associated thrombosis: the when, how and why. *Eur Respir Rev*. 2019;28(151):180119. doi:10.1183/16000617.0119-2018
3. Blom JW, Doggen CJ, Osanto S, Rosendaal FR. Malignancies, prothrombotic mutations, and the risk of venous thrombosis. *JAMA*. 2005;293(6):715–722. doi:10.1001/jama.293.6
4. Khorana AA, Connolly GC. Assessing risk of venous thromboembolism in the patient with cancer. *J Clin Oncol*. 2009;27(29):4839–4847. doi:10.1200/jco.2009.22.3271
5. Girardi L, Wang T-F, Ageno W, Carrier M. Updates in the incidence, pathogenesis, and management of cancer and venous thromboembolism. *Arteriosclerosis Thrombosis Vasc Biol*. 2023;43(6):824–831. doi:10.1161/ATVBAHA.123.318779
6. Khorana AA, Mackman N, Falanga A, et al. Cancer-associated venous thromboembolism. *Nat Rev Dis Primers*. 2022;8(1):11. doi:10.1038/s41572-022-00336-y
7. Key NS, Khorana AA, Kuderer NM, et al. Venous thromboembolism prophylaxis and treatment in patients with cancer: ASCO clinical practice guideline update. *J Clin Oncol*. 2020;38(5):496–520. doi:10.1200/jco.19.01461
8. Ay C, Beyer-Westendorf J, Pabinger I. Treatment of cancer-associated venous thromboembolism in the age of direct oral anticoagulants. *Ann Oncol*. 2019;30(6):897–907. doi:10.1093/annonc/mdz111
9. Steffel J, Verhamme P, Potpara TS, et al. The 2018 European heart rhythm association practical guide on the use of non-vitamin K antagonist oral anticoagulants in patients with atrial fibrillation. *Eur Heart J*. 2018;39(16):1330–1393. doi:10.1093/eurheartj/ehy136
10. Patel MR, Mahaffey KW, Garg J, et al. Rivaroxaban versus warfarin in nonvalvular atrial fibrillation. *N Engl J Med*. 2011;365(10):883–891. doi:10.1056/NEJMoa1009638
11. Granger CB, Alexander JH, McMurray JJ, et al. Apixaban versus warfarin in patients with atrial fibrillation. *N Engl J Med*. 2011;365(11):981–992. doi:10.1056/NEJMoa1107039
12. Mcbane RD, Mcbane Ii R, Loprinzi CL, et al. Apixaban and dalteparin in active malignancy associated venous thromboembolism. The ADAM VTE trial. *Thrombosis Haemostasis*. 2017;117(10):1952–1961. doi:10.1160/TH17-03-0193
13. Giancarlo A, Cecilia B, Rupert B, et al. Apixaban versus dalteparin for the treatment of acute venous thromboembolism in patients with cancer: the caravaggio study. *Thrombosis Haemostasis*. 2018;118:s–0038–1668523.
14. Young AM, Marshall A, Thirlwall J, et al. Comparison of an oral factor xa inhibitor with low molecular weight heparin in patients with cancer with venous thromboembolism: results of a randomized trial (SELECT-D). *J Clin Oncol*. 2018;36(20):JCO2018788034. doi:10.1200/JCO.2018.78.8034
15. Kraaijpoel N, Nisio MD, Mulder FI, Es NV, Raskob GE. Clinical impact of bleeding in cancer-associated venous thromboembolism: results from the Hokusai VTE cancer study. *Thrombosis Haemostasis*. 2018;118(8):1439–1449. doi:10.1055/s-0038-1667001
16. Bertoletti L, Ollier E, Duvillard C, et al. Direct oral anticoagulants: current indications and unmet needs in the treatment of venous thromboembolism. *Pharmacol Res*. 2017;118:33–42. doi:10.1016/j.phrs.2016.06.023
17. Wang Z, Li Y, He X, et al. In vivo evaluation of the pharmacokinetic interactions between almonertinib and rivaroxaban, almonertinib and apixaban. *Front Pharmacol*. 2023;14:1263975. doi:10.3389/fphar.2023.1263975
18. Bellesoeur A, Thomas-Schoemann A, Allard M, et al. Pharmacokinetic variability of anticoagulants in patients with cancer-associated thrombosis: clinical consequences. *Crit Rev Oncol/Hematol*. 2018;129:102–112. doi:10.1016/j.critrevonc.2018.06.015
19. Nair A, Morsy MA, Jacob S. Dose translation between laboratory animals and human in preclinical and clinical phases of drug development. *Drug Dev Res*. 2018;79(8):373–382. doi:10.1002/ddr.21461
20. Administration, U. S. D. o. H. a. H. S. F. a. D. Population pharmacokinetics guidance for industry. 2022. Available from: https://www.fda.gov/media/128793/download. Accessed August 19, 2025.
21. M10 bioanalytical method validation and study sample analysis guidance for industry. 2022. Available from: https://www.fda.gov/regulatory-information/search-fda-guidance-documents/m10-bioanalytical-method-validation-and-study-sample-analysis. Accessed August 19, 2025.

22. Arifin WN, Zahiruddin WM. Sample size calculation in animal studies using resource equation approach. *Malays J Med Sci*. 2017;24(5):101–105. doi:10.21315/mjms2017.24.5.11
23. Nebert DW, Russell DW. Clinical importance of the cytochromes P450. *Lancet*. 2002;360(9340):1155–1162. doi:10.1016/s0140-6736(02)11203-7
24. Benet LZ, Cummins CL. The drug efflux-metabolism alliance: biochemical aspects. *Adv Drug Deliv Rev*. 2001;50 Suppl 1:S3–11. doi:10.1016/s0169-409x(01)00178-8
25. Frost CE, Byon W, Song Y, et al. Effect of ketoconazole and diltiazem on the pharmacokinetics of apixaban, an oral direct factor Xa inhibitor. *Br J Clin Pharmacol*. 2015;79(5):838–846. doi:10.1111/bcp.12541
26. Kim M, Son H, Noh K, Kim E, Shin BS, Kang W. Effects of verapamil and diltiazem on the pharmacokinetics and pharmacodynamics of rivaroxaban. *Pharmaceutics*. 2019;11(3). doi:10.3390/pharmaceutics11030133
27. Dhillon S. Palbociclib: first global approval. *Drugs*. 2015;75(5):543–551. doi:10.1007/s40265-015-0379-9
28. Zhao T, Chen Y, Wang D, et al. Identifying the dominant contribution of human cytochrome P450 2J2 to the metabolism of rivaroxaban, an oral anticoagulant. *Cardiovasc Drugs Ther*. 2022;36(1):121–129. doi:10.1007/s10557-020-07129-z
29. Olie RH, Winckers K, Rocca B, Ten Cate H. Oral anticoagulants beyond warfarin. *Annu Rev Pharmacol Toxicol*. 2024;64(1):551–575. doi:10.1146/annurev-pharmtox-032823-122811
30. Crawley RM, Anderson RL. Prevention and treatment of bleeding with direct oral anticoagulants. *Drugs*. 2020;80(13):1293–1308. doi:10.1007/s40265-020-01345-5
31. Li M, Xiao J, Yu T, et al. Analysis of hemorrhagic drug-drug interactions between P-gp inhibitors and direct oral anticoagulants from the FDA adverse event reporting system. *Expert Opin Drug Saf*. 2024;1–9. doi:10.1080/14740338.2024.2376693
32. Vasilogianni AM, Al-Majdoub ZM, Achour B, Peters SA, Rostami-Hodjegan A, Barber J. Proteomics of colorectal cancer liver metastasis: a quantitative focus on drug elimination and pharmacodynamics effects. *Br J Clin Pharmacol*. 2022;88(4):1811–1823. doi:10.1111/bcp.15098
33. Cvan Trobec K, Kerec Kos M, Trontelj J, et al. Influence of cancer cachexia on drug liver metabolism and renal elimination in rats. *J Cachexia Sarcopenia Muscle*. 2015;6(1):45–52. doi:10.1002/jcsm.12012
34. (CDER), U. S. D. o. H. a. H. S. F. a. D. A. C. f. D. E. a. R. In vitro drug interaction studies — cytochrome P450 enzyme- and transporter-mediated drug interactions guidance for industry. 2020. Available from: https://www.fda.gov/regulatory-information/search-fda-guidance-documents/in-vitro-drug-interaction-studies-cytochrome-p450-enzyme-and-transporter-mediated-drug-interactions. Accessed August 19, 2025.